

PDF SIMULATION OF TURBULENT SPRAY FLOWS

Hai-Wen Ge and Eva Gutheil

Interdisziplinäres Zentrum für Wissenschaftliches Rechnen
Ruprecht-Karls-Universität Heidelberg
Im Neuenheimer Feld 368, 69120 Heidelberg
Germany

ABSTRACT

A probability density function (PDF) method is extended to turbulent spray flows. The PDF transport equation of the gas-phase mixture fraction for turbulent spray flows is deduced, modeled and solved. The numerical results of the methanol vapor mass fraction for a non-reacting spray, which are obtained using the PDF method, are in good agreement with experimental data and improve the ones from the moment closure method. Furthermore, the shapes of the probability density function of the mixture fraction at different positions, which are computed by Monte-Carlo method, are presented and analyzed. It appears that the spray source changes the value of the mean mixture fraction, but it does not change the shape of its PDF. A comparison of the Monte-Carlo PDF with the standard β PDF shows the standard β function to fail to describe the shape of the PDF. With the definition of appropriate local maximum and minimum values of the mixture fraction, a modified formulation of the β PDF is suitable to reflect the shape of the Monte-Carlo PDF very well.

1. INTRODUCTION

Turbulent spray flows are frequently encountered in industrial processes such as internal engine combustion, gas-turbine combustors, liquid-fueled furnaces, and aircraft propulsion. Their numerical prediction is valuable for both theoretical studies and engineering purposes. When chemical reactions are involved in the turbulence, the computational cost becomes very high because of the high degree of freedom of the system of governing equations. For 3D flows with N chemical species, the degree of freedom is $N+4$. With the flamelet model [1] where the mixture fraction and its variance are used to compute the chemical composition of the gas phase, the degree of freedom is reduced to seven. Moreover, the stiffness problem in computation of chemical reaction is also avoided. The flamelet model is widely used in turbulent gas diffusion flames [2,3]. Hollmann *et al.* [4,5] extended it to turbulent spray evaporation and combustion systems.

In the flamelet model the mixture fraction's statistical distribution usually is described by a two-parameter β function [1-5]. The β function gives good numerical results for gas-phase flows. However, results from direct numerical simulations (DNS) show that it fails in the evaporation region of the gas-liquid flow [6]. The distribution of the mixture fraction does not follow the β PDF in regions where vaporization exists. Therefore, the assumed β PDF should be assessed before being used in the turbulent spray flows. In the present work, the transport equation of the PDF (noted as PDF method in the remainder of the paper) is used to exert the statistical distribution of the mixture fraction in the turbulent spray flow. The PDF method is a powerful tool to simulate the turbulent flows [7]. It treats the term for convection, mean pressure gradient, source (including the chemical reaction and the vaporization source terms) exactly whereas the molecular diffusion term and the fluctuating pressure gradient term need modeling. Advantages of the method are that all moments of the variables can be determined. Moreover, the Lagrangian PDF takes full account of long memory of turbulence. The computational cost of the PDF method compared to direct numerical simulations is considerably lower.

The PDF method was introduced by Lundgren [8] for the turbulent velocity field and by Dopazo *et al.* [9] for the gas composition. It became very popular since Pope's work [7]. In the past 10 years, the PDF method was extended to simulate multi-phase flows. Raju [10] and Taut *et al.* [11] describe the gas phase in turbulent two-phase flows with the PDF transport equation. Zhu *et al.* [12] and Rumberg *et al.* [13] deduced and solved the joint PDF transport equation of all liquid-phase and gas-phase dependent variables. Liu *et al.* [14] deduced and solved the joint PDF transport equation of the properties of droplets and gas eddies seen by droplets.

The objective of the present work is the analysis of the statistical distribution of the gas-phase mixture fraction in turbulent spray flows. The PDF method is implemented to simulate the gas phase in turbulent spray flows. The PDF transport equation of the mixture fraction in turbulent spray flows is deduced and solved. In the next section, the governing equations and models are presented. In section 3, the numerical method is described in detail. In section 4, the numerical results of PDF method are compared with experimental data [15] and results from moment closure method [4,5]. The PDF of mixture fraction computed by Monte-Carlo method is compared with assumed standard β PDF and modified β PDF. Finally, the paper concludes with an assessment of the current PDF method and presumed PDF of a scalar in the turbulent spray flow.

2. MATHEMATICAL MODEL

The one-point one-time Eulerian, Favre-averaged probability density function $\tilde{f}(\xi_c; \vec{x}, t)$ of the mixture fraction is defined as

$$\tilde{f}(\xi_c; \vec{x}, t) = \rho(\xi_c) \langle (\xi_c - \xi_c) \rangle / \langle \rho \rangle. \quad (1)$$

According to the transport equation of the instantaneous mixture fraction in a turbulent spray flow,

$$\frac{\partial(\rho \xi_c)}{\partial t} + \frac{\partial(\rho U_j \xi_c)}{\partial x_j} = \frac{\partial}{\partial x_j} \left(\rho D_M \frac{\partial(\xi_c)}{\partial x_j} \right) + \dot{\rho}^s, \quad (2)$$

the PDF transport equation of mixture fraction \tilde{f} is deduced following the way suggested by Pope [7]:

$$\bar{\rho} \frac{\partial \tilde{f}}{\partial t} + \bar{\rho} U_j \frac{\partial \tilde{f}}{\partial x_j} + \frac{\partial(\bar{\rho} \bar{S}_s \tilde{f})}{\partial \xi_c} = - \frac{\partial}{\partial \xi_c} \left[\bar{\rho} \left\langle \frac{\partial}{\partial x_j} \left(D_M \frac{\partial \xi_c}{\partial x_j} \right) \right| \xi_c \right] \tilde{f}. \quad (3)$$

Here $\bar{S}_s = \bar{\rho}^s / \bar{\rho}$ denotes the averaged source term due to droplet evaporation. $U_j = \tilde{U}_j + u_j$ denotes the instantaneous gas velocity in j -direction. The terms on the left-hand side in Eq. (3) can be solved exactly. The term on the right-hand side representing the transport in mixture fraction space by molecular fluxes, needs to be modeled. Here the simplest model, the Interaction-by-Exchange-with-the-Mean (IEM) model [7], is used to account the effects of molecular diffusion. The evolution equation of particles' mixture fraction is written as

$$\frac{d\xi_c(t)}{dt} = - \frac{1}{2} \frac{\tilde{\varepsilon}}{\bar{k}} C_\phi \left[\xi_c(t) - \hat{\xi}_c \right] + \bar{S}_s. \quad (4)$$

For the closure of the PDF transport equations, the conservation equations of gas flow including the extended $k - \varepsilon$ model [17] are solved. Considering a steady, two-dimensional, axi-symmetric, turbulent liquid jet with no swirl, the Favre-averaged governing equations of a gas flow can be written as

$$L(\tilde{\Phi}) \equiv \frac{\partial(\bar{\rho} \tilde{U}_i \tilde{\Phi})}{\partial x_i} - \frac{\partial}{\partial x_i} \left(\Gamma_{\Phi, \text{eff}} \frac{\partial \tilde{\Phi}}{\partial x_i} \right) = \bar{L}_{\text{gas}, \tilde{\Phi}} + \bar{L}_{\text{spray}, \tilde{\Phi}}. \quad (5)$$

The conservation variables $\tilde{\Phi}$ and source terms of the gas phase $\bar{L}_{\text{gas}, \tilde{\Phi}}$ and the liquid phase $\bar{L}_{\text{spray}, \tilde{\Phi}}$ are described in detail in [4].

The spray is represented by a finite number of droplet parcels. Each parcel contains a number of droplets with the same location, size, velocity and temperature [4]. Assuming a dilute spray, droplet-droplet interaction is neglected. Only drag force and gravity are considered. The effect of gas-phase turbulence on droplet velocities is modeled using the stochastic-separated-flow (SSF) model [16]. The instantaneous gas velocity is computed by a Monte-Carlo method. The distribution of the velocity fluctuating is assumed to be a Gaussian distribution [4]. The droplet heating for methanol at atmospheric pressure is modeled using the infinite-conductivity model. This model is appropriate for the small droplet size and the fuel methanol with its relatively high volatility at atmospheric pressure. The Abramzon-Sirignano model [17] is used to calculate the evaporation rate of droplets in a convective flow field. The properties in the gas film surrounding the droplet are determined according to the 1/3 rule [18].

3. NUMERICAL METHOD

A finite-volume method based on SIMPLE algorithm is used to solve Eqs. (5). It provides the mean variables that appear in the evolution equations of droplets and gas particles. The Lagrangian particle method is employed to determine droplets' position, velocity, temperature, and size. The source terms due to spray evaporation are fed back to the finite-volume method code and gas-phase Monte-Carlo code using the Particle-Source-In-Cell model [4]. The PDF transport equation of the mixture fraction is solved by a Lagrangian Monte-Carlo method. The one-point PDF is represented by a finite number of gas particles. Each gas particle has a set of properties $\{m^*, \vec{x}^*, \xi_c^*\}$. The gas particle with the coordinate \vec{x}^* evolves according to

$$\frac{d\vec{x}^*(t)}{dt} = \vec{U}(\vec{x}^*(t)) + \vec{u}^*(\vec{x}^*(t)). \quad (6)$$

The fluctuating velocity \vec{u}^* is determined from the turbulent kinetic energy using the Monte-Carlo method. The mixture fraction of gas particles evolves according to Eq. (4). The Favre-averaged mean variables \vec{U} , \bar{k} , and $\tilde{\varepsilon}$ appearing in Eq. (4) and Eqs. (6-9), are computed by the finite-volume scheme and then they are linearly interpolated to the particle/droplet's position. The value of $\hat{\xi}_c$ in Eq. (4) is determined using the cloud-in-cell method [19]. A second-order algorithm [19] is used to solve Eq. (6). At each time step, new gas particles are supplied at the inlet. At the solid wall boundary as well as the axis of symmetry the particles are reflected. If particles move out of computational domain, they are discarded. To reduce the statistical error in the result of Monte-Carlo method, a time-averaging scheme is implemented [19].

4. RESULTS AND DISCUSSION

A steady, two-dimensional, axi-symmetric, non-reactive turbulent liquid jet without swirl is modeled. A dilute methanol spray is injected into turbulent air. Experiments were performed by McDonnell and Samuelsen [15]. The geometry of the fuel injector is found in [15]. We mark the section of the fuel injector's exit as $x = 0$ mm. The gas and droplet velocities, droplet size distribution, liquid flux and concentration of methanol vapor are measured at the axial location $x = 7.5$ mm, 25mm, 50mm, 100mm.

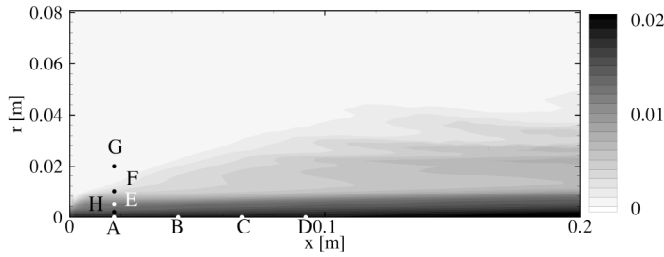


Fig. 1: Contour plot of the methanol vapor mass fraction. Positions show the points where the PDF is studied.

The experimental data at $x = 7.5$ mm are taken as inlet profiles for numerical computations. At the inlet, the top-hat profile is prescribed for the gas particles' mixture fraction. The average number of gas particle per cell is set to 80.

Figure 1 shows the contour plot of the Favre-averaged fuel vapor mass fraction computed by the PDF method. The positions A-H marked in the figure are used to evaluate the probability density functions discussed in Figs. (3)-(7).

The major vaporization occurs near the nozzle where the differences of temperature, velocity between droplets and gas flow are relatively large. The most methanol vapor is transported along the axis of symmetry by the jet while the rest develops into radial direction. Further downstream, vaporization becomes weak.

Experimental data for the methanol vapor mass fraction as well as the axial gas velocity are available at the axial positions of $x = 25$ mm, 50 mm, 75 mm, 100 mm, and 150 mm. Figure 2 shows the mean profiles at the first two positions where the experiments [15] are compared to results from the moment closure method [4,5] and PDF method. The results of PDF method are in good agreement with experimental data, and they improve the ones obtained by moment closure method in the initial region. In the moment closure method, the mixture fraction is calculated by solving the Favre-averaged conservation equation. The effects of turbulent transport are modeled by introducing a kinematic eddy viscosity $\mu_t = c_\mu \bar{k}^2 / \bar{\epsilon}$. In the PDF transport equation, the effects of turbulent transport are taken into account through a Monte-Carlo method, which improves the physical mechanism. The deviation of the results of the PDF method is mainly due to the $k-\epsilon$ model used in finite-volume code. The $k-\epsilon$ model under-predicts the periodic fluctuation of the gas velocity. Consequently, the moment exchange in the lateral direction is under-predicted, and the spreading rate of the jet is over-predicted. As a result in velocity field, the axial velocity at the axis of symmetry is under-predicted, especially in the region close to nozzle (see Fig. 2 left). This implies that the methanol vapor transported to the axis of symmetry is under-predicted. The droplets presenting at the axis of symmetry are also under-predicted. Both of these two effects result in the under-prediction of the mass fraction of methanol vapor near the axis of symmetry. Therefore, the results of the PDF method could be improved if the velocity field was more accurate.

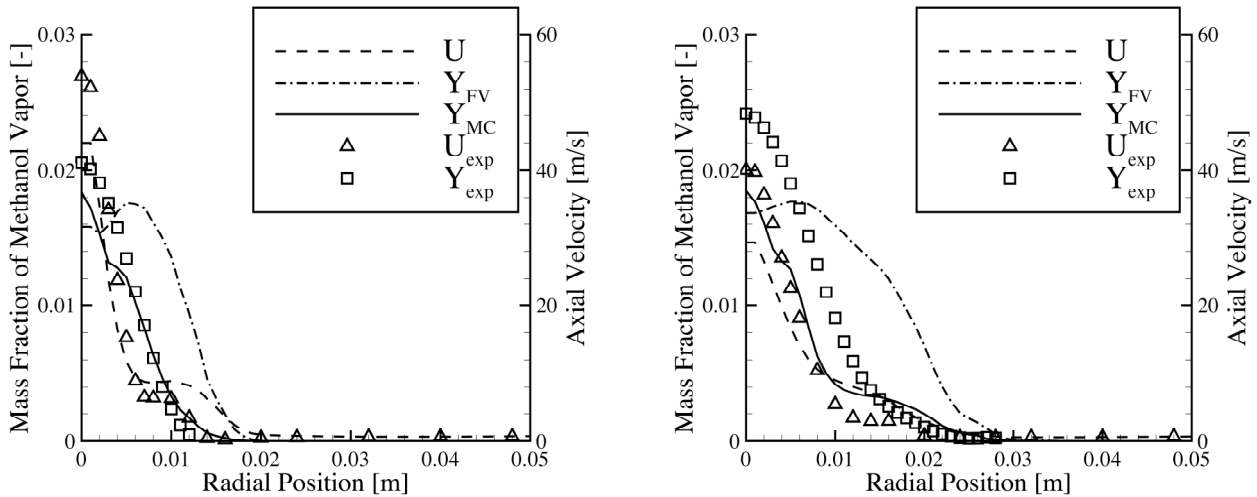


Fig. 2: Mean profiles of the Favre-averaged axial gas velocity, U , and the fuel vapor mass fraction, Y , at an axial position of $x = 25$ mm (left) and $x = 50$ mm (right) obtained by the Monte-Carlo (MC) and the moment closure (FV) methods, respectively, and from experiment (exp).

Figures 3-4 show the probability density function of mixture fraction at different positions, which are marked in Fig. 1. Along the axial line, all of the PDFs show a bimodal shape (see Fig. 3). The variance of mixture fraction becomes smaller along the axial line. The fluctuation of the scalar is larger at the upstream because of stronger turbulent fluctuation there. As a result, the left peak gets weaker at the downstream (see Fig. 3 position C and D). When the local fluctuation is small enough, the PDF will have a Gaussian-like shape. It will become a delta function when the variance is close to zero. Along the radial line (see Fig. 4), the positions A, F, G are located in the region of the main vaporization zone, weak vaporization and pure air. The fluctuation of mixture fraction is weaker in the outside region than in the inner region. The variance of mixture fraction along the radial line decreases with increasing radial distance r . As a consequence, the PDF of the mixture fraction evolves from bimodal to unimodal,

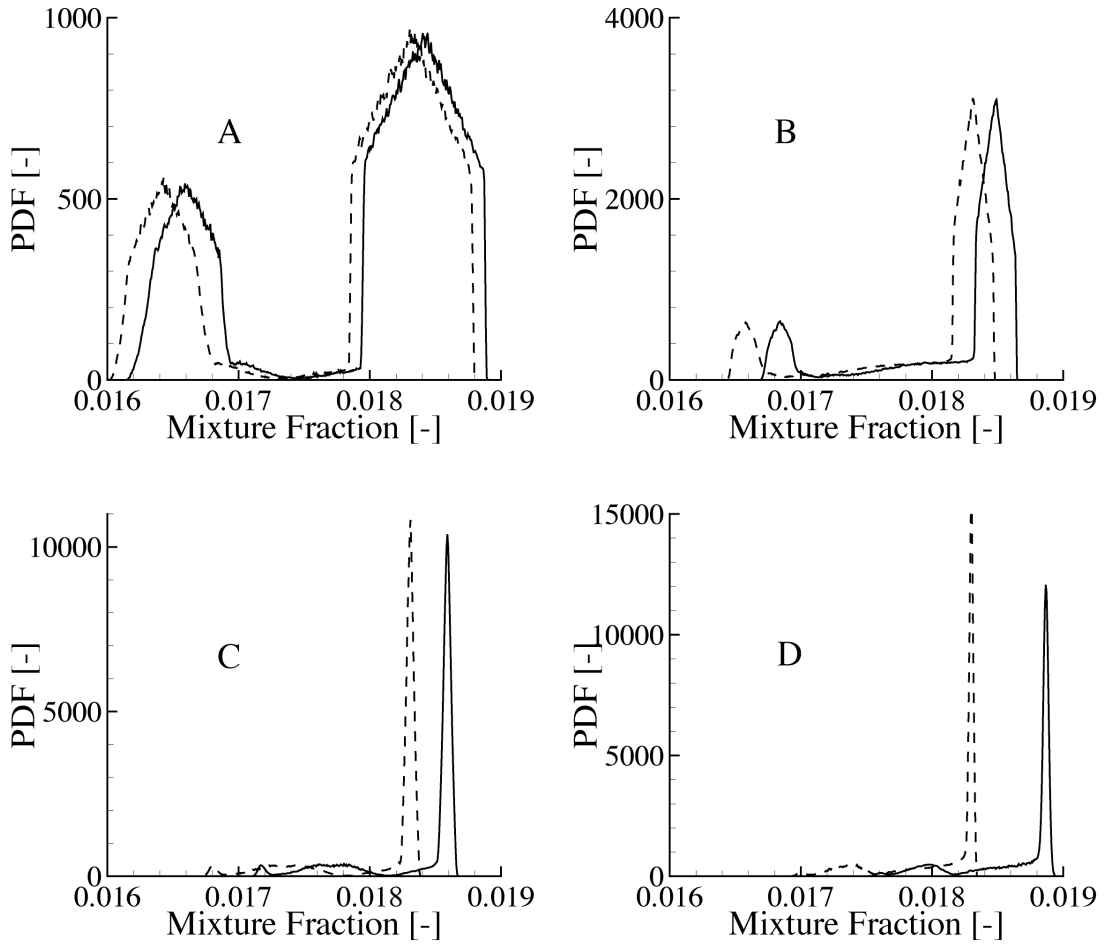


Fig. 3: PDFs of the mixture fraction, positions at central line; dashed lines indicate the case with spray source term set to zero.

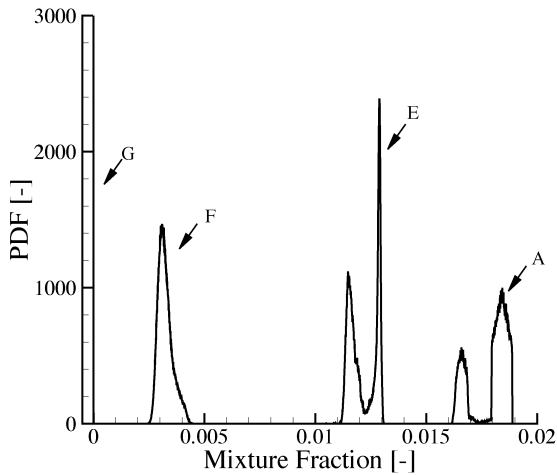


Fig. 4: PDFs of the mixture fraction, radial line.

and to a delta function in the region of pure air (position G). The value of the PDF at G extends to a very high value to satisfy the normalization condition of the PDF, and it is cut off in the figure.

To assess the effect of spray source on the PDF of mixture fraction, the same calculation is performed where the spray source is set to zero. All other flow characteristics including density, velocity, turbulent kinetic energy and its dissipation rate, are kept the same. The PDFs along the central line indicated by dash-line is presented in Fig. 3. Compared to the case with spray source (solid line in Fig. 3), the principal shape of PDFs does not change. The mean value of mixture fraction is reduced. According to Eq. (4), the difference of the mean mixture fraction is $\Delta \tilde{\xi}_c = -(2/C_\phi)(\tilde{k}/\tilde{\epsilon})\bar{S}_s$ compared to the case with spray source.

Figures. 5-7 show the comparison of the assumed PDF and the PDF computed by the Monte-Carlo method (solid lines). The assumed PDFs used here are the standard β PDF (β_1 in the figures)

$$P(\xi_c) = \frac{\Gamma(\alpha + \beta)}{\Gamma(\alpha)\Gamma(\beta)} \xi_c^{\alpha-1} (1 - \xi_c)^{\beta-1}, \quad (11)$$

and the following suggested modified β PDF (β_2 in the figures)

$$P(\xi_c) = \frac{\Gamma(\alpha + \beta)}{\Gamma(\alpha)\Gamma(\beta)} (\xi_{c,max} - \xi_{c,min})^{1-\alpha-\beta} (\xi_c - \xi_{c,min})^{\alpha-1} (\xi_{c,max} - \xi_c)^{\beta-1}. \quad (12)$$

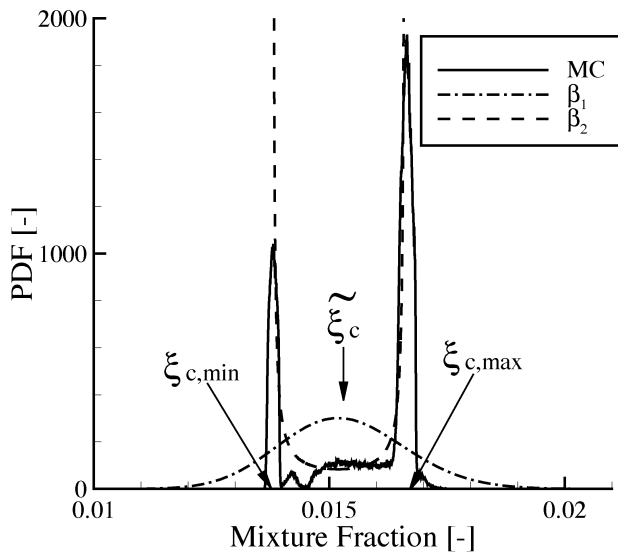


Fig. 5: Comparison of standard (1) and modified (2) β PDF computed with the Monte-Carlo method (MC), Position H. The positions of $\xi_{c,max}$ and $\xi_{c,min}$ are used in the modified β PDF.

The symbol ξ_c in the figures indicates the position of the mean value of mixture fraction computed by the Monte-Carlo method. The values of $\xi_{c,max}$ and $\xi_{c,min}$ are indicated on the axis of mixture fraction by arrows in Figs. 5-7. With the mean and the variance of mixture fraction computed by the Monte-Carlo method, the standard β PDF (c.f. Eq. (11)) can be determined. However, the standard β PDF always shows Gaussian-like (unimodal) distribution for the conditions of the current flow field as shown in the figures. This shape does not represent the computed Monte-Carlo PDF, in particular when the PDF of mixture fraction shows a bimodal shape (see Figs. 5 and 6). With the same mean and variance of mixture fraction from Monte-Carlo method, and local maximum and minimum values of mixture fraction $\xi_{c,max}$ and $\xi_{c,min}$, the modified β PDF (c.f. Eq. (12)) can be determined. With appropriate values of $\xi_{c,max}$ and $\xi_{c,min}$, the modified β PDF represents the computed Monte-Carlo PDF very well. Even when the computed PDF shows a Gaussian-like shape (see Fig. 7), the modified β PDF still performs very well. It should be mentioned that the standard β PDF is a special form of the modified β PDF with $\xi_{c,max} = 1$ and $\xi_{c,min} = 0$.

The predictive ability of the standard β PDF in turbulent spray flow mainly depends on the value of $(1-\xi_{c,max})$ and $(\xi_{c,min}-0)$. In the current situation, these deviations are quite large. Assuming that the spray stream has reached the saturation, the maximum mass fraction of methanol vapor at the droplet surface is roughly 0.1. The corresponding mixture fraction is 0.1 which is considerably smaller than unity. Therefore, the standard β PDF is far away from the Monte-Carlo PDF. When the value of the local $\xi_{c,max}$ and $\xi_{c,min}$ are close enough to unity and zero, respectively, the standard β PDF is reasonable to give good estimations to the Monte-Carlo PDF of the mixture fraction.

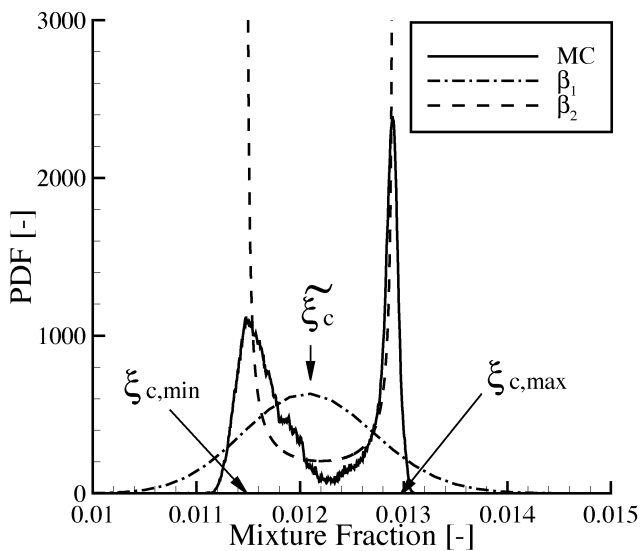


Fig. 6: Comparison of standard (1) and modified (2) β PDF computed with the Monte-Carlo method (MC), Position H. The positions of $\xi_{c,max}$ and $\xi_{c,min}$ are used in the modified β PDF.

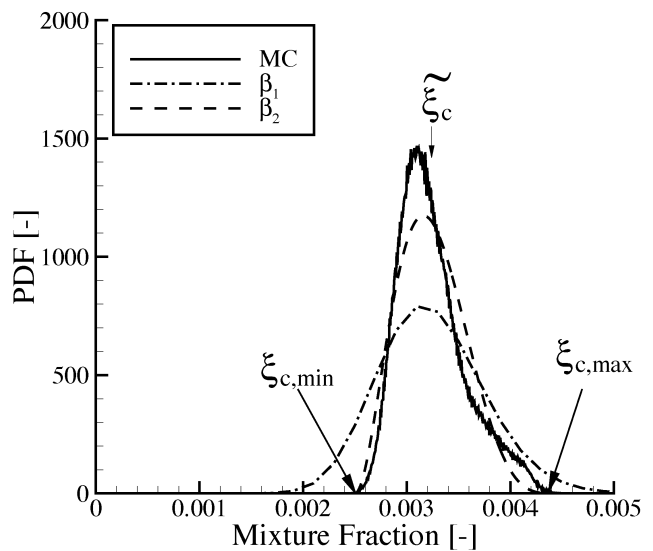


Fig. 7: Comparison of standard (1) and modified (2) β PDF computed with the Monte-Carlo method (MC), Position H. The positions of $\xi_{c,max}$ and $\xi_{c,min}$ are used in the modified β PDF.

5. CONCLUSIONS

In the present work, the PDF (Probability Density Function) method is used to model a steady, 2D, axi-symmetric, turbulent methanol/air spray flow without swirl. The PDF transport equation is formulated and then solved by a hybrid finite-volume method and a Lagrangian Monte-Carlo method. The numerical results of the PDF method are in a good agreement with experimental data. The comparison shows the PDF method to improve the results computed by moment closure method. It is demonstrated that the PDF method is suitable to predict the characteristics of turbulent spray flows with some under-prediction concerning the methanol vapor fraction in radial direction further downstream.

The PDF of mixture fraction at different position in turbulent spray flow is presented. It is found that the spray source only changes the mean of the mixture fraction, but it does not change the principal shape of the PDF of mixture fraction. The PDF of mixture fraction computed by Monte-Carlo method is compared with the presumed β PDF. The standard β PDF fails to describe the Monte-Carlo PDF. With appropriate local maximum and minimum values of mixture fraction, a modified β PDF represents the results of the computed PDF very well.

In the future work, the turbulent reactive spray flows will be investigated.

ACKNOWLEDGEMENT

The authors gratefully acknowledge the financial support from DFG through Graduiertenkolleg "Complex Processes: Modeling, Simulation and Optimization", IWR, Universität Heidelberg.

REFERENCES

1. N. Peters, Turbulent Combustion, Cambridge University Press, Cambridge, 2000.
2. N. Peters, The Use of Flamelet Models in CFD-Simulations, *ERCOFTAC Bulletin*, no. 38, pp.71-78, 1999.
3. H. Pitsch, Unsteady Flamelet Modeling of Differential Diffusion in Turbulent Jet Diffusion Flames, *Combust. Flame*, vol.123, pp.358-374, 2000.
4. C. Hollmann and E. Gutheil, Modelling of Turbulent Spray Diffusion Flames Including Detailed Chemistry, *Proc. Combust. Inst.*, vol.26, pp.1731-1738, 1996.
5. C. Hollmann and E. Gutheil, Flamelet-Modelling of Turbulent Spray Diffusion Flames Based on a Laminar Spray Flame Library, *Combust. Sci. Tech.*, vol.135, no.1-6, pp.175-192, 1998.
6. R.S. Miller and J. Bellan, On the Validity of the Assumed Probability Density Function Method for Modeling Binary Mixing/Reaction of Evaporated Vapor in Gas/Liquid-Droplet Turbulent Shear Flow, *Proc. Combust. Inst.*, vol.27, pp.1065-1072, 1998.
7. S.B. Pope, PDF Methods for Turbulent Reactive Flows, *Prog. Energy Combust. Sci.*, vol.11, pp.119-192, 1985.
8. T.S. Lundgren, Model Equation for Non-homogeneous Turbulence, *Phys. Fluids*, vol.12, pp.485-497, 1969.
9. C. Dopazo and E.E. O'Brien, An Approach to the Autoignition of a Turbulent Mixture. *Acta. Astronaut.*, vol.1, pp.1239-1266, 1974.
10. M.S. Raju, Application of Scalar Monte Carlo Probability Density Function Method for Turbulent Spray Flames, *Numer. Heat Trans., Part A*, vol.30, no.8, pp.753-777, 1996.
11. C. Taut, C. Correa, O. Deutschmann, J. Warnatz, S. Eimecke, C. Schulz and J. Wolfrum, 3D-Modeling with Monte-Carlo-PDF Methods and Laser Diagnostics of the Combustion in a Two-Stroke Engine, *Proc. Combust. Inst.*, vol.28, pp.1153-1159, 2000.
12. M. Zhu, K.N.C. Bray and B. Rogg, PDF Modeling of Spray Autoignition in High Pressure Turbulent Flows, *Combust. Sci. Tech.*, vol.120, no.1-6, pp.357-379, 1996.
13. O. Rumberg and B. Rogg, Full PDF Modeling of Reactive Sprays via an Evaporation-Progress Variable, *Combust. Sci. Tech.*, vol.158, pp.211-247, 2000.
14. Z.H. Liu, C.G. Zheng and L.X. Zhou, A Joint PDF Model for Turbulent Spray Evaporation/Combustion, *Proc. Combust. Inst.*, vol.29, pp.561-568, 2002.
15. V.G. McDonnell and G.S. Samuelsen, An Experimental Data Base for Computational Fluid Dynamics of Reacting and Nonreacting Methanol Sprays, *J. Fluids Engin.*, vol.117, pp.145-153, 1995.
16. G.M. Faeth, Evaporation and Combustion of Sprays, *Prog. Energy Combust. Sci.*, vol.9, pp.1-76, 1983.
17. B. Abramzon and W.A. Sirignano, Droplet Vaporization Model for Spray Combustion Calculation, *Int. J. Heat Mass Transfer*, vol.9, pp.1605-1618, 1989.
18. G.L. Hubbard, V.E. Denny and A.F. Mills, Droplet Evaporation: Effects of Transients and Variable Properties, *Int. J. Heat Mass Transfer*, vol.18, no.9, pp.1003-1008, 1975
19. P. Jenny, S.B. Pope, M. Muradoglu, and D.A. Caughey, A Hybrid Algorithm for the Joint PDF Equation of Turbulent Reactive Flows, *J. Comp. Phys.*, vol.166, pp.218-252, 2001.